IEEE Transactions on Nuclear Science, Vol. NS-26, No. 3, June 1979

INFORMATION FROM BEAM RESPONSE TO LONGITUDINAL AND TRANSVERSE EXCITATION

J. Borer, G. Guignard, A. Hofmann, E. Peschardt, F. Sacherer† and B. Zotter *

Summary

The response of a beam to small longitudinal or transverse excitation defines its "beam transfer function" (BTF). The BTF is the inverse of the stability diagram[1,2,3] and is affected by phenomena such as Landau damping, the chamber wall impedance, active feedback systems, and non-linear resonances. The contribution of each phenomenon is extracted from the BTF. Measurement of the working line in the presence of a stack and the monitoring of instabilities is performed by suitable processing of the BTF. These measurements have a completely negligible effect on the beam quality and may therefore even be performed during periods of "stable beams". The BTF technique has been implemented in the transverse plane in a set-up involving a dual-channel fast Fourier transform (FFT) spectrum analyser. This set-up allows fast measurement of the BTF from white noise excitation of the beam. Typical examples of actual measurements are given.

1. Introduction

The spectra of the statistical fluctuations of the current of coasting beams in storage rings are known as the natural Schottky scans. They have been extensively used since 1972 in the CERN ISR to monitor the radial density distribution, to measure the Q values at the beam edges and to detect the growth of the transverse beam dimensions[4]. This technique has been improved using a dual channel FFT spectrum analyser which measures a given spectrum up to 800 times faster than the conventional spectrum analysers hitherto in use[5]. Furthermore the FFT spectrum analyser allows the measurement of transfer functions by low-level white noise excitation of the beam. A new monitoring system has been built to derive and analyse the transverse BTFs.

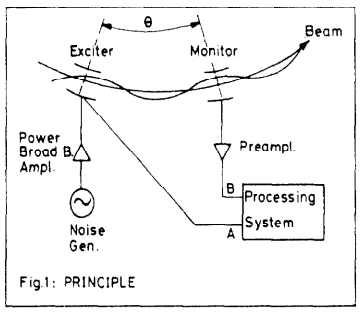

Fig.1: PRINCIPLE

2. Theory of Coasting Beam Transfer Functions

2.1 Transverse case

Given the theoretical block diagram of Fig. 1, the transfer function of a beam is its response to a transverse periodic acceleration $G\,e^{-i\omega t}$ (part of the wide spectrum of the exciter). The motion of a single particle in the absence of self forces is given by

$$\frac{dx^2}{dt^2} + Q^2\Omega^2 x = G\,e^{-i\omega t} \qquad (1)$$

with x = transverse excursion, $\Omega/2\pi$ = revolution frequency and Q the betatron wave number (which is assumed to depend only on the momentum p) of the particle. Assuming a wave solution $x = x_0 \exp[i(n\theta-\omega t)]$ and using the relation $\frac{d}{dt} = \frac{\partial}{\partial t} + \Omega\frac{\partial}{\partial\theta} = i(n\Omega-\omega)$ we find the response seen by a detector at a fixed position θ:

$$\frac{x_o}{G} = \frac{\exp(-in\theta)}{\Omega^2Q^2-(n\Omega-\omega)^2} = \frac{-\exp(-in\theta)}{[\omega-\Omega(n+Q)][\omega-\Omega(n-Q)]} \qquad (2)$$

From now on a detector close to the exciter (θ = 0) will be chosen. The response (2) is only large if the exciting frequency ω is either $\omega \approx \Omega(n_f+Q) = \omega_{\beta f}$ (exciting the fast wave) or $\omega \approx \Omega(n_s-Q) = \omega_{\beta s}$ (exciting the slow wave). The displacement $\bar{x}$ of the centre of charge of many particles N, having the distributions $F_f(\omega_{\beta f})$ and $F_s(\omega_{\beta s})$ (with $\int F(\omega_\beta)d\omega_\beta = N$) in fast and slow wave frequencies, is obtained by averaging over the displacements of the single particles

$$\left(\frac{\bar{x}}{G}\right)_{(f/s)} = \frac{(-/+)}{2\Omega_o Q_o N}\int \frac{F(\omega_\beta)d\omega_\beta}{\omega-\omega_\beta} = \frac{(-/+)}{2\Omega_o Q_o N}\left[PV+i\pi F(\omega)\right] \qquad (3)$$

where the -/+ sign refers to the fast/slow wave and the index "o" to the values in the centre of the distribution. The dispersion integral appearing in (3) has a real "principal value" (PV) and an imaginary residue (the sign of the latter refers to a growing solution[6]). We can simplify by replacing ω_β and ω by relative frequencies ξ and ξ_1 which are normalized with the HWHM (half width half max.) frequency spread S and also using a normalized distribution f(x) [6].

$$f(\xi) = \frac{S}{N}F(\omega_\beta) \quad \text{with} \quad \int f(\xi)d\xi = 1 \qquad (4)$$

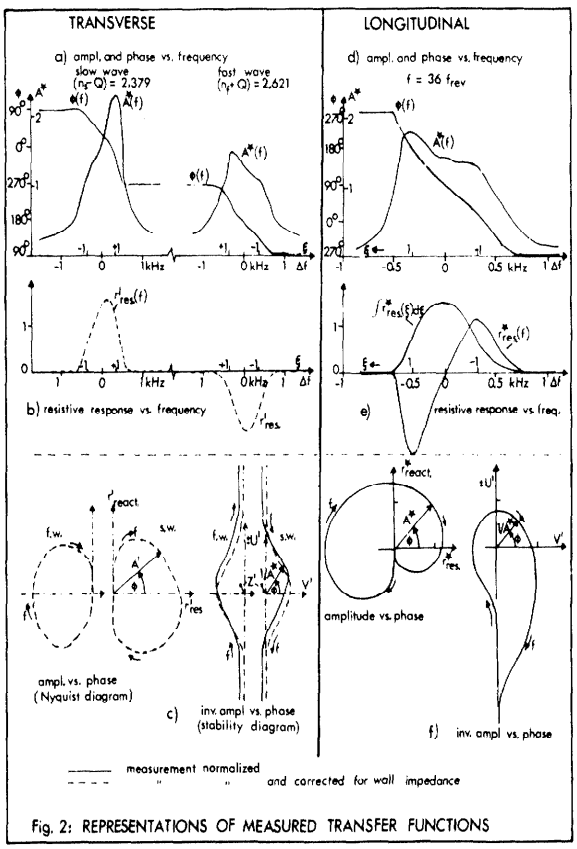

Fig. 2: REPRESENTATIONS OF MEASURED TRANSFER FUNCTIONS

* CERN, Geneva, Switzerland

Furthermore it is more relevant to know the responding velocity $\dot{\bar{x}} = -i\omega\bar{x}$ than the displacement since the absorbed power is proportional to $\dot{\bar{x}} \cdot G$. The absolute magnitude of this response is usually difficult to measure but can be calibrated from the known quantities S and N by using the relation (4) leading to a normalized response.

$$r'_{(f/s)} = \frac{\dot{\bar{x}}}{G} \frac{2\Omega_0 Q_0 S}{\omega} = (-/+) \left[\pi f(\xi_1) + iPV\right] \quad (5)$$

The inverse response $1/r'$ is usually called the stability diagram.

The transverse wall impedance Z_T [7] will introduce an additional acceleration G_Z due to the beam-induced, transversely-acting fields $\vec{E}$ and $\vec{B}$.

$$G_Z = \frac{e \int_0^{2\pi R} \left[\vec{E} + (\vec{\beta} c \times \vec{B})\right]_T ds}{2\pi R m_0 \gamma} = \frac{iec\Omega_0 I_0 Z_T \bar{x}}{2\pi m_0 c^2 \gamma} = i2S\Omega_0 Z'_T \bar{x}$$

where R is the average radius of the machine, I_0 the total beam current and Z'_T the normalized impedance (Z'_T is a complex, dimensionless quantity). This acceleration G_Z has to be added to G in (1) leading to a final inverse response $1/r^*$

$$\left(\frac{1}{r^*}\right)_{(f/s)} = \frac{(-/+)}{\pi f(\xi_1) + iPV} - Z' = \frac{1}{r'} - Z'_T \quad (6)$$

The transverse impedance shifts the stability diagram by $-Z'_T$. This allows the measurement of the complex wall impedance [3,7] or the "impedance" of a feedback system to check its proper adjustment (Figs. 4 and 5). Furthermore equation (6) allows the correction of a measured response (Fig. 2a) for the effect of a known impedance (Fig. 2c) to obtain r' (Fig. 2b). The resistive part of r' gives with (5) the distribution $f(\xi)$ and with (4) the real distribution $F(\omega_\beta)$ in incoherent betatron frequencies.

With the FFT analyser we can excite the beam simultaneously at many frequencies (white noise) and obtain the response at once over the whole spectrum. For a linear system this response is identical to that obtained with a swept frequency.

2.2 Longitudinal case

The response to a longitudinal periodic excitation $G\, e^{-i\omega t}$ can be calculated in a similar way [8] leading to a normalized response:

$$r'_L = \pi \frac{df(\xi_1)}{d\xi} + i \int \frac{\frac{df(\xi)}{d\xi} d\xi}{\xi_1 - \xi} \quad (7)$$

where ξ and ξ_1 are the corresponding harmonic revolution frequencies or momentum deviations normalized with the corresponding longitudinal spread S_L discussed in detail in reference 6. A measured longitudinal response in phase and amplitude is shown in Fig. 2d and the corresponding stability diagram in Fig. 2f. The resistive part of r' is proportional to the derivative of the longitudinal particle distribution $f(\xi)$ and the distribution itself is obtained by integration (Fig. 2e). The longitudinal impedance had a very small effect in the example shown and no correction has been made for it.

3. Equipment Description

A block diagram of the set-up is shown in Fig. 3. The transverse monitors are electrostatic pick-ups (PUs) followed by very low noise tuned amplifiers for the Schottky spectra and wideband amplifiers for the BTFs. The longitudinal beam signals are collected by a wideband gap monitor, or wideband coaxial transformer, with a shunt resistance of 1Ω. The transverse exciters are identical to the transverse PUs. The signals are selected with coaxial relays and fed to a dual channel frequency shifter acting as a mixing-down converter. This converter which is controlled by a synthesiser has an input frequency range from 100 kHz to 100 MHz and an output frequency band, selectable in seven steps from 0-1 kHz to 0-100 kHz in order to match the FFT spectrum analyser. The white noise source used to excite the beam has a bandwidth of 300 kHz. It is generated by mixing up a white noise source from 0-300 kHz to the frequency band selected by the synthesiser for the frequency shifter. The response of the beam is fed to the FFT spectrum analyser together with the exciting noise and the BTF is calculated. The result is displayed on two screens and transmitted to a computer for further treatment.

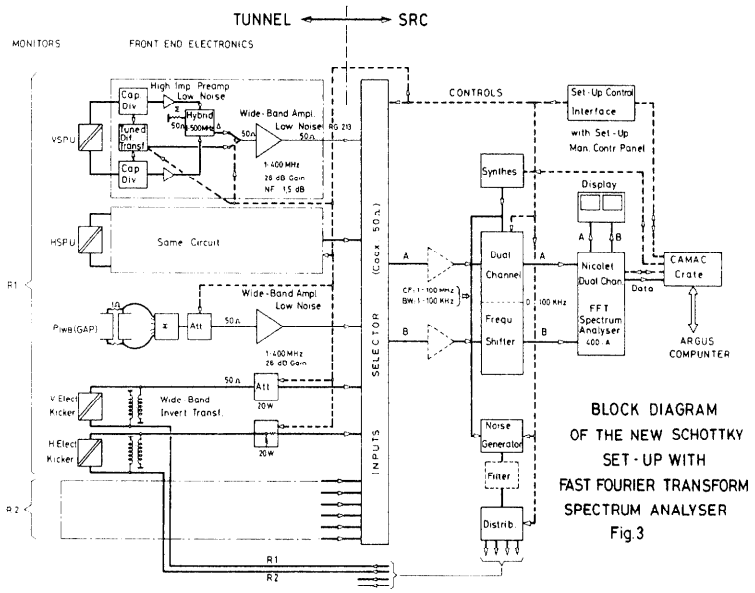

4. Measurement Examples on Actual Stacks

4.1 The influence of transverse feedback

Figure 4 shows an example of a vertical BTF of a 20 A stack at 26 GeV/c. In one case the 50 MHz feedback system for stabilising vertical transverse instabilities is switched on and in the other it is off. From the BTF the stability diagram has been calculated. The result is plotted in Fig. 5 where the vectors due to the wall impedance and the transverse feedback are indicated (relative scale).

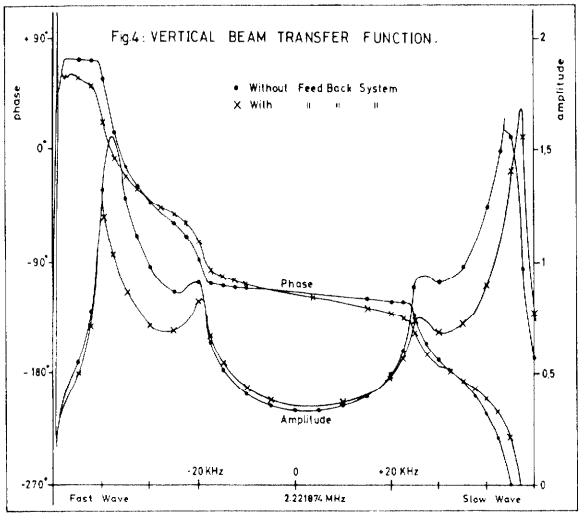

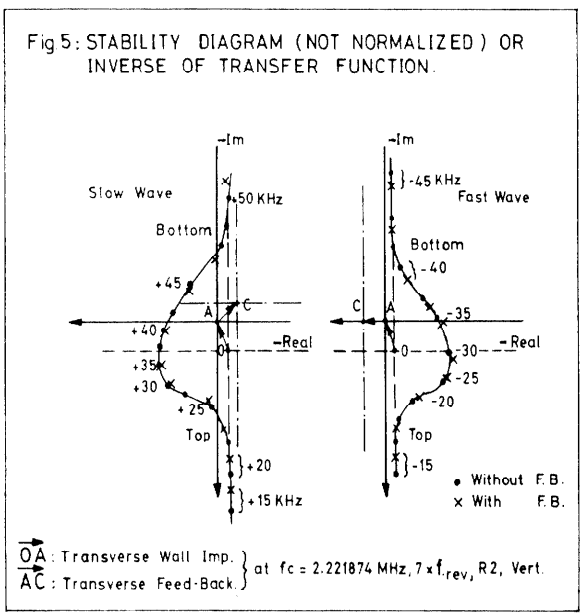

4.2 Resonance excitation

For the purpose of this experiment a special working line was created which crossed the fourth order resonance $4Q_H = 35$. The strength of this resonance can be controlled by correct powering of a set of compensating octupoles[9].

A stack was then made on the generated working line. The BTF was measured and showed peaks at frequencies corresponding to the resonance even with the octupoles switched off. The strength of the 4th order resonance was then increased (octupoles at +20%) and the BTF remeasured (see Fig. 6). The form of this

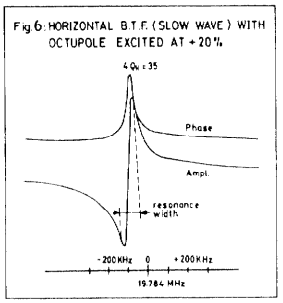

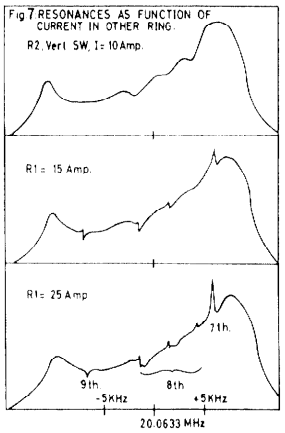

response can be explained by resonance mechanisms[10]. The betatron amplitude of those particles trapped on the resonance grows with time. However, due to the non-linear fields (e.g. octupoles) the tune of the particle is amplitude-dependent. Consequently the increase in betatron amplitude causes a tune change which moves the particle out of resonance. The loss of particles on resonance creates a hole in the amplitude of the response while the tune shift with amplitude creates a peak to one side of the resonance. This side should depend on the sign of the non-linear frequency shift, the dominant component being the octupole zero harmonic. The distance between the hole and the peak (the resonance width) should vary with this zero harmonic and with the resonance strength (Fig. 6). The measured resonance width ($\Delta Q_H = 1.8 \cdot 10^{-4}$) from Fig. 6 is roughly equal to the bandwidth[10] ($\Delta e \cong 2 \cdot 10^{-4}$) calculated from the octupole excitation. The peak in the phase of the response gives the decimal part of the tune at resonance within 10^{-4}, with the scale of Fig. 6 ($q_H = 0.74997$).

4.3 Beam-beam induced resonances

In another experiment, high-order resonances were observed with the FFT in a 10 A stack on the ELSA line. Figure 7 shows that resonances of order ≥ 7 due to magnetic field imperfections are not visible, while beam-beam resonances of order 7 to 9 start to appear with 15 A in the other ring. Increasing the current of the exciting beam up to 25 A shows that resonances are enhanced, that coupled resonances such as $2Q_H + 6Q_V$ appear and that even a 15th order resonance may become visible. The vertical beam-beam tune shift deduced from these measurements is equal to -0.0001 per ampere in the stack centre.

Fig. 8 shows an example of the BTF polar plot of a 31 GeV/c, 28 A beam influences by a similar beam in the other ring. Fig. 9 shows the real part projection as function of frequency where resonances due to non-linear vertical fields are clearly visible. Such resonances also exist in the horizontal plane but are of much smaller amplitude and barely visible on the BTF. However,

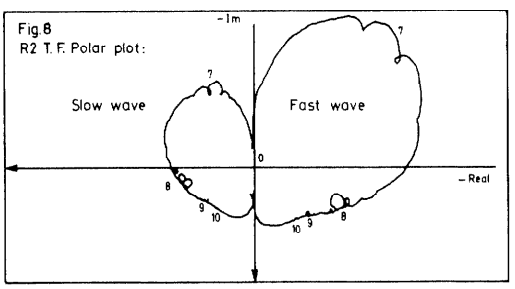

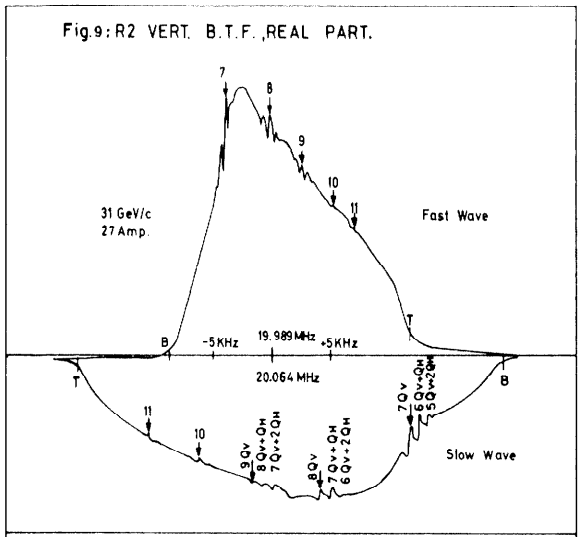

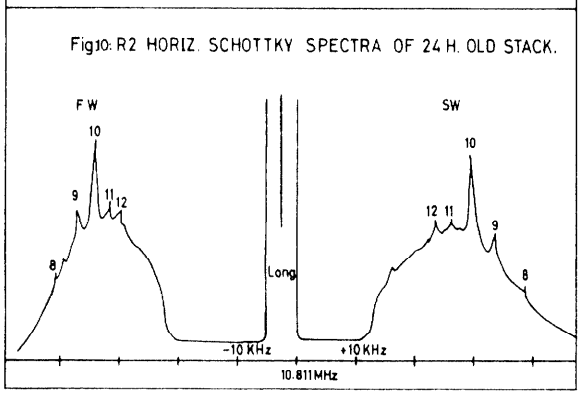

their cumulative effect is not negligible as can be seen on the "natural" Schottky scan after 24 h (Fig. 10). The positions of these vertical and horizontal resonances are indicated in the Q_V-Q_H diagram (Fig. 11). They coincide well with the intersection between the diagram resonance lines and the actual working line as calculated out of the BTF real part or transverse distributions.

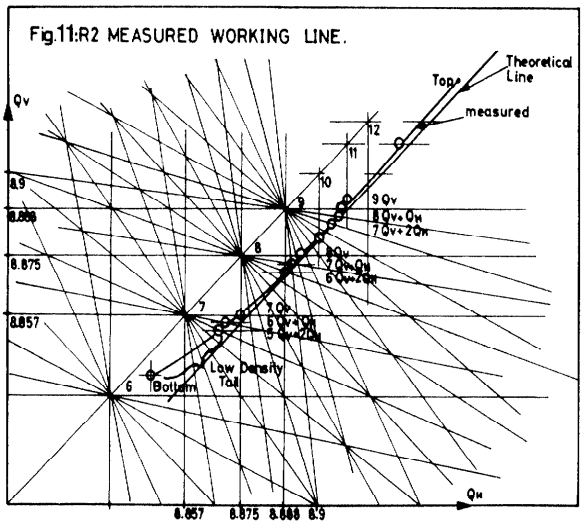

5. Future Developments

This new equipment and measuring technique combining FFT processing and noise excitation to produce the beam transfer function, is a powerful tool for monitoring the beam behaviour in storage rings during operation. This technique has no measurable disturbing effect on the beam and therefore can be used during ISR physics time. The BTF computer processing for obtaining the working line, the distributions and emittances, wall and feedback systems' impedances etc. are being implemented. The same equipment can also be used for the measurement of phase advance, for beam-beam interactions, linear coupling and stochasticity limits etc.

Acknowledgements

Thanks are due to Messrs D. Cocq, J.-C. Juillard, D. Kemp and H. Verelst for the design and construction of the equipment hardware and software. We thank Messrs S. Myers, L. Thorndahl and E.H. Smith (Birmingham University) for very useful comments and contributions to the theoretical aspects of the subject, and Mr J.-Y. Hemery for help in programming.

References

1. H. Grunder and G. Lambertson, Transverse Beam Instabilities at the Bevatron, Proc. Internat. Conf. on High Energy Accelerators, CERN 1971, pp. 308-9, 1971.
2. D. Möhl and A. Sessler, The Use of RF-KO for Determination of the Characteristics of the Transverse Coherent Instability of an Intense Beam, Proc. Internat. Conf. on High Energy Accelerators, CERN 1971, pp. 334-7, 1971.
3. A. Hofmann and B. Zotter, Measurement of Beam Stability and Coupling Impedance by RF Excitation, IEEE Trans. Nucl. Sci. NS-24, No. 3, pp. 1487-9, 1977.
4. J. Borer, P. Bramham, H.G. Hereward, K. Hübner, W. Schnell and L. Thorndahl, Non-destructive diagnosis of Coasting Beams with Schottky Noise, Proc. Internat. Conf. on High Energy Accelerators, Stanford 1974, pp. 53-6, 1974.
5. A. Sabersky, Private communication, May 1975.
6. K. Hübner and V. Vaccaro, Dispersion Relation and Stability of Coasting Beams, CERN Internal Report, ISR/TH/70-44, 1970.
7. W. Schnell, Coherent Instabilities of Proton Beams in Accelerators and Storage Rings - Experimental Results, Diagnosis and Cures, CERN Report 77-13, pp. 231-5, 1977.
8. A. Faltens, E.C. Hartwig, D. Möhl and A.M. Sessler, An Analog Method for Measuring the Longitudinal Coupling Impedance of a Relativistic Particle Beam with its Environment, Proc. Internat. Conf. on High Energy Accelerators, CERN 1971, pp. 338-344, 1971.
9. J.-P. Gourber, Control of Betatron Frequencies and of resonance excitation in the ISR, Proc. 4th All-Union Nat. Conf. on Particle Accelerators, Moscow, 1974, vol. 2, pp. 73-76, 1975.
10. G. Guignard, A General Treatment of Resonances in Accelerators, CERN Report 78-11, 1978.